Destabilization of F-actin by Mechanical Stress Deprivation or Tpm3.1 Inhibition Promotes a Pathological Phenotype in Tendon Cells

Kameron L. Inguito[1], Mandy M. Schofield[1], Arya D. Faghri[1], Ellen T. Bloom[2], Marissa Heino[1,2], Dawn M. Elliott[2], Justin Parreno*[1,2]

[1]Department of Biological Sciences, University of Delaware, Newark, DE

[2]Department of Biomedical Engineering, University of Delaware, Newark, DE

Correspondence:

Justin Parreno (Email: jparreno@udel.edu)

Address: Biological Sciences, Wolf Hall, 105 The Green, Newark, DE, 19716

Abstract

The actin cytoskeleton is a central mediator between mechanical force and cellular phenotype. In tendon, it is speculated that mechanical stress deprivation regulates gene expression by filamentous (F-) actin destabilization. However, the molecular mechanisms that stabilize tenocyte F-actin networks remain unclear. Tropomyosins (Tpms) are master regulators of F-actin networks. There are over 40 mammalian Tpm isoforms, with each isoform having the unique capability to stabilize F-actin sub-populations. Thus, the specific Tpm(s) expressed by a cell defines overall F-actin organization. Here, we investigated F-actin destabilization by stress deprivation of tendon and tested the hypothesis that stress fiber-associated Tpm(s) stabilize tenocyte F-actin to regulate cellular phenotype. Stress deprivation of mouse tail tendon fascicles downregulated tenocyte genes (collagen-I, tenascin-C, scleraxis, α-smooth muscle actin) and upregulated matrix metalloproteinase-3. Concomitant with mRNA modulation were increases in DNAse-I/Phallodin (G/F-actin) staining, confirming F-actin destabilization by tendon stress deprivation. To investigate the molecular regulation of F-actin stabilization, we first identified the Tpms expressed by mouse tendons. Tendon cells from different origins (tail, Achilles, plantaris) express three isoforms in common: Tpm1.6, 3.1, and 4.2. We examined the function of Tpm3.1 since we previously determined that it stabilizes F-actin stress fibers in lens epithelial cells. Tpm3.1 associated with F-actin stress fibers in native and primary tendon cells. Inhibition of Tpm3.1 depolymerized F-actin, leading to decreases in tenogenic expression, increases in chondrogenic expression, and enhancement of protease expression. These expression changes by Tpm3.1 inhibition are consistent with tendinosis progression. A further understanding of F-actin stability in musculoskeletal cells could lead to new therapeutic interventions to prevent alterations in cellular phenotype during disease progression.

Introduction

The dysregulation of filamentous (F-) actin is associated with a wide range of pathologies in load-bearing mechanical tissues [1-10]. While the complete interactions between mechanical forces, F-actin, and pathology are not fully clear, the actin cytoskeleton may be a key mediator between mechanical force and cellular phenotype[1, 7, 11-14]. Tendon is an ideal tissue model to examine the mechanical regulation of cellular phenotype [15]. Mechanical loading of tendon is essential to maintain tissue homeostasis and tissue overloading is a cause of tendinosis [16-22]. While it may be speculated that tendon overload leads to mechanical over-stimulation of residing tendon cells, leading to alterations in cell phenotype (i.e., MMP production) [15, 23], an alternative hypothesis is that overload leads to a paradoxical mechanical under stimulation or stress deprivation of tendon cells [24, 25]. The hypothesized disruption of cell-matrix interactions during overload results in the failure of loads to be transmitted to cells. In support of this hypothesis, overloading of rat tail tendon resulted in cell-matrix disruptions as demonstrated using transmission electron microscopy by an increase in spacing between matrix and cells [26].

Mechanical loading/unloading of explant tendon tissue has been widely used to investigate the connection between cellular stress deprivation and tissue degeneration. Unloading or stress depriving tendons by culturing explants in the absence of mechanical load, recapitulates several aspects of tendinosis. Stress deprivation alters tendon cell phenotype causing a reduction in tendon molecule (such as collagen 1; Col1) expression and enhancement of matrix degradation molecule (such as matrix metalloproteinases; Mmps) expression as compared to tendons freshly isolated from a mechanically stressed *in vivo* environment [27-36]. However, stretching tendons while in culture prevents these tendinosis-like changes. The protective effects of stretch are abrogated if tendons are cultured in the presence of F-actin depolymerization agent, cytochalasin D, while

being stretched [13, 37]. These findings have led to the speculation that stress deprivation regulates tendon cell phenotype via F-actin destabilization. This destabilization leads to depolymerization of F-actin into monomeric, globular (G-) actin which has been shown in other cell types to regulate gene expression [38-41]. However, there is limited data to support that stress deprivation destabilizes/depolymerizes F-actin. In the present study, we ask: is F-actin depolymerized during tendon stress deprivation? To answer this, we performed whole-mount confocal imaging followed by image quantification to compare freshly isolated stress-deprived tendons stained for F- and G-actin. We confirm that the acquisition of tendinosis-like molecular expression by stress deprivation correlates with F-actin destabilization.

Our finding of F-actin destabilization prompted us to examine the molecular regulation of F-actin network stability in tendon cells. We focused on the regulation of F-actin networks by tropomyosin (Tpm), the master regulator of F-actin that binds along and stabilizes F-actin [42]. The regulation of tenocyte F-actin by Tpms is largely unknown. In native and *in vitro* (primary cultured) tendon cells, F-actin organizes into stress fibers [14] containing alpha-smooth muscle actin (αsma), a highly contractile form of actin [11, 14, 43, 44]. Tpm associates with F-actin stress fibers in tendon cells [14]. However, the particular Tpm(s) expressed within tendon cells are not clear. Over forty isoforms of mammalian tropomyosin exist and each isoform has the unique capability to stabilize specific F-actin sub-populations. Thus, the particular Tpm(s) expressed within a cell defines overall F-actin organization.

In this study, we aim to determine which Tpm isoforms are expressed by tendon cells. Since tenocyte F-actin networks arrange into stress fibers, we focused on elucidating the function of stress fiber-associated Tpm isoforms. Previous studies using osteosarcoma (U2OS) cells have indicated at least six Tpms (1.6, 1.7, 2.1, 3.1, 3.2 and 4.2) are associated with stress fibers [45, 46].

93 In lens epithelial cells, we demonstrated that inhibition of just one Tpm isoform (Tpm3.1) prevents
94 stress fiber formation resulting in downstream gene modulation [38]. Therefore, in this study we
95 tested the hypothesis that stress fiber-associated Tpm(s) stabilize tenocyte F-actin and regulate
96 cellular phenotype by modulating mRNA levels.

97 It is essential to unravel how cellular phenotype is determined by the F-actin network's
98 response to mechanical forces and to elucidate the molecules that determine/stabilize F-actin
99 networks. Establishing the mechanisms involved in regulating cellular phenotype by F-actin in
100 pathological processes, such as tendon overload, could lead to new therapeutic opportunities
101 against disease.

102

103

104 **Methods**

105 *Mice and tissue isolation*

106 Wild-type mice, 8-10 weeks of age, in the C57BL/6J background were used for
107 experiments. All procedures were conducted following approved animal protocols from the
108 University of Delaware. Following euthanasia, plantaris, Achilles, and tail tendons were isolated
109 as previously described [47-49]. To dissect plantaris and Achilles tendons, approximately 1 cm of
110 the plantaris and Achilles complex were removed with the calcaneus intact. The tendons were
111 separated by removing excess surrounding soft tissue before cutting off the calcaneal insertion
112 [47]. Tail tendon fascicles were obtained from excised tails using forceps [48].

113

114 *Tendon explant stress deprivation culture*

115 Tendon stress deprivation was performed by placing isolated tendon fascicles in culture
116 vessels submerged in serum-free DMEM (GenClone, Genesee Scientific, San Diego, CA, USA)
117 consisting of 1% antimycotic/antibiotic (MilliporeSigma, Burlington, MA, USA) [28, 33, 36, 50].
118 Tendons were maintained at 37ºC and 5% CO_2 and were harvested at set time points, either 1- or
119 2-days post-isolation. For these studies, tail tendon fascicles were distributed in a non-biased
120 fashion to experimental conditions, with freshly isolated fascicles serving as controls.

121

122 *Tail tenocyte isolation and Tpm3.1 inhibition by TR100 treatment*

123 To obtain tendon cells, tail tendon fascicles were isolated and immersed in 0.2%
124 Collagenase A (MilliporeSigma) and maintained at 37ºC. Following overnight incubation, digests
125 were strained through 100µm filters and then centrifuged at 600g for 6 minutes. Tenocyte pellets
126 were resuspended in fresh DMEM consisting of 10% fetal bovine serum (FBS; GenClone) and 1%

127 antimycotic/antibiotic. For experiments, cells were counted and then seeded on culture vessels at
128 a density between 5 to10 x 10^3cells/cm^2. Every two days spent media was replaced with fresh
129 media. Once tenocyte cultures reached ~70% confluency, cells were serum starved in DMEM
130 consisting of 0.5%FBS and 0.1% antimycotic/antibiotic with or without Tpm3.1 inhibitor (TR100;
131 1-10μM; MilliporeSigma). Tendon cells were harvested 1-or 2-days after drug treatment.
132
133 *Light microscopy and cell area/circularity quantification*
134 Following 24 hours of treatment, cells were imaged using a microscopy camera (Swiftcam
135 Technologies, Hong Kong) attached to an Axiovert 25 inverted phase-contrast microscope (Zeiss,
136 Jena, Germany). The boundaries of individual cells were manually traced on images using FIJI
137 software. Cell area and circularity were calculated using FIJI software algorithms as previously
138 performed [39]. Circularity was defined as $C = 4\pi(A/P^2)$ where, P is the perimeter, and A is the
139 cell area. A circularity value of 0 indicates an elongated elipse, whereas a value of 1 indicates a
140 perfect circle.
141
142 *Cell viability assay*
143 We used a propidium iodide exclusion assay to quantify the proportion of live cells
144 following TR100 treatment. Cells on culture vessels were placed in 0.05% trypsin at 37ºC. After
145 5 minutes, cells were centrifuged, and pellets were then resuspended in PBS containing 0.5μg/mL
146 propidium iodide. Propidium iodide is impermeable to live cells but incorporates into dead cells
147 with compromised cell membranes. A Tali Image-based Cytometer (ThermoFisher Scientific;
148 Waltham, MA) was used to calculate the portion of cells in suspension that incorporated propidium
149 iodide. Cells exposed to 70% ethanol served as dead controls.

150 For visualization of cell viability, cells on culture vessels were stained with 1μM Calcein
151 AM (live cell stain) and 1μM propidium iodide in PBS at 37ºC. After 10 minutes, cells were rinsed
152 with PBS and visualized using a Zeiss Axio Observer 7 microscope. Cells fixed in 4%
153 paraformaldehyde (before staining) were used as dead cell control.
154
155 *RNA isolation, gene expression, and Tpm sequencing*
156 For RNA processing, tendon tissue or cultured tendon cells were immersed in TRIzol
157 (Sigma-Aldrich, Burlington, MA) and stored frozen until further use. To extract RNA from tissues,
158 tissues were manually grinded in TRIzol using a Pellet Pestle. RNA was separated via phase
159 separation with chloroform, followed by selective recovery of total RNA using an RNA spin
160 column clean-up kit (RNA Clean & Concentrator-5; Zymo, Irvine, CA). RNA was extracted from
161 cultured cells by phase separation with chloroform followed by RNA precipitation in isopropanol
162 as previously described [38]. Reverse transcription of RNA to cDNA was performed using
163 UltraScript 2.0 cDNA Synthesis Kit (PCR Biosystems, Wayne, PA).
164 Semi-quantitative RT-PCR was performed using PCRBIO Taq Mix Red solution (PCR
165 Biosystems; London, UK) on equivalent amounts of cDNA using previously validated Tpm
166 primers [51]. PCR products were run on a 2% Agarose gel. Gel bands were excised, melted, and
167 DNA was purified using GenCatch Advance Gel Extraction Kit (Epoch Life Sciences; Missouri
168 City, TX, USA). Purified DNA was sequenced using Sanger sequencing (Genewiz, South
169 Plainfield, NJ, USA).

170 Relative real-time RT-PCR was performed using qPCRBio Sygreen Blue Mix (PCR
171 Biosystems, Wayne, PA) according to manufacturer's directions. Each reaction contained 20ng of
172 cDNA in a 10µL volume using primers that are listed in Table 1. Real-time PCR was conducted
173 on a Cielo 3 PCR machine (Azure; Houston, TX, USA).

Table 1. List of Real-time RT-PCR Primers

Gene	Forward Primer	Reverse Primer	Product Size (bp)	Accession No.
18S	GCAATTATTCCCCATGAACG	GGCCTCACTAAACCATCCAA	123	NR_003278.3
αsma	TCACCATTGGAAACGAAC	CCCCTGACAGGACGTTGTTA	162	NM_007392.3
Acan	GAAAACTTCGGGGTGGG	TCCCTCTGTGACATTACGGG	96	NM_007424.3
Col1	AGCACGTCTGGTTTGGAGAG	GACATTAGGCGCAGGAAGGT	112	NM_007742.4
Mmp-3	GGTGACCCCACTCACTTTCT	GGCATGAGCCAAGACTGTTC	124	NM_010809.2
Mmp-13	AGACCCCAACCCTAAGCATC	ATAGGGCTGGGTCACACTTC	53	NM_008607.2
Scx	CCACTGAAGAGTCACGGAGA	CTGTTCATAGGCCCTGCTCA	111	NM_198885.3
Sox9	AGTACCCGCATCTGCACAAC	TACTTGTAATCGGGGTGGTCTT	145	NM_011448.4
Tnc	TGGAATTGCTCCCAGCATCC	CCGGTTCAGCTTCTGTGGTAG	65	NM_011607.3

174

175 *Wes capillary electrophoresis*

176 Total protein was extracted as previously described [38] with slight modifications. Briefly,
177 protein was extracted in 1x Radioimmunoprecipitation (RIPA) lysis buffer (Millipore Sigma) and
178 then quantified using a bicinchoninic acid protein assay (BCA) (Prometheus Protein Biology
179 Products; Genesee Scientific, San Diego, CA, USA). Specific protein levels were determined using
180 a WES Capillary-Based Electrophoresis assay with a 12-230 kDa separation module kit following
181 the manufacturer instructions (Protein Simple, San Jose, CA, USA) with an equal volume of
182 control and experimental protein. The antibodies used for experiments are rabbit anti-pan-Actin
183 (1:100; #4968, Cell Signaling), mouse anti-αSMA (1:50; ab7817, Abcam), and rabbit anti-MMP-
184 3 (1:10; EP1186Y, Abcam). Secondary antibodies used were anti-rabbit or anti-mouse HRP-
185 conjugate (Protein Simple). Specific protein levels were normalized to total protein. Total protein

186 values were determined using a Chemiluminescent WES Simple Western Size-Based Total Protein
187 Assay (Protein Simple).
188
189 *Immunostaining of native tendon*
190 Whole tendons were placed in 4% paraformaldehyde in phosphate-buffered saline (PBS;
191 GenClone) at 4ºC for 2 hours. Fixed tendons were then washed three times in PBS and incubated
192 in permeabilization/blocking buffer (PBS containing 0.3%Triton, 0.3% bovine serum albumin, and
193 3% goat serum) at room temperature. After 2 hours, tendons were transferred into a primary
194 antibody solution containing 1:100 mouse anti-Tpm3.1 antibody (2G10.2; Millipore Sigma) in
195 permeabilization/blocking solution. After overnight incubation at 4ºC, tendons were washed six
196 times in PBS and placed in secondary antibody solution containing fluorescent CF488 anti-mouse
197 secondary antibody (1:200; Biotium, Fremont, CA), Hoecsht 33342 (1:500; Biotium), and
198 rhodamine-phalloidin (1:20; Biotium) in permeabilization/blocking buffer at room temperature for
199 2 hours in the dark. Tissues were then washed six times in PBS, placed on a glass slide, and
200 mounted using ProLong gold anti-fade reagent (Thermo Fisher Scientific).
201 To stain for G/F-actin, fixed tendons were placed in permeabilization/blocking buffer at
202 room temperature. After 2 hours, tendons were transferred into permeabilization/blocking buffer
203 containing Hoecsht 33342 (1:500), Alexa Fluor DNAse-I (Thermo Fisher Scientific) and
204 rhodamine-phalloidin (1:20).
205
206 *Immunostaining of cultured cells*
207 Tendon cells cultured on glass-bottomed dishes (World Precision Instruments, Sarasota,
208 FL, USA) were fixed with 4% paraformaldehyde in PBS at room temperature. After 10 minutes,

209 fixed cells were washed in PBS and kept at 4ºC. Tendon cells were immunostained by first
210 incubating in permeabilization/blocking buffer at room temperature for 30 minutes. Next, cells
211 were incubated with mouse anti-TPM3.1 antibody (1:200; 2G10.2, MilliporeSigma) or rabbit anti-
212 SCX antibody (1:100; ab58655, Abcam) diluted into permeabilization/blocking solution. After
213 overnight incubation at 4ºC, cells were washed six times in PBS and placed in secondary antibody
214 solution containing CF488 anti-mouse secondary antibody (1:200), Hoechst 33342 (1:500) to stain
215 nuclei, and rhodamine-phalloidin (1:50) to stain F-actin, in permeabilization/blocking buffer at
216 room temperature for 1 hour in the dark. Cells were then washed six times in PBS and mounted
217 using ProLong gold anti-fade reagent (Thermo Fisher Scientific).
218
219 *Confocal fluorescence microscopy*
220 Stained tissues and cells were imaged using a Zeiss LSM880 laser-scanning confocal fluorescence
221 microscope (Zeiss) using a 20x 0.8NA objective or a 63x 1.4NA oil objective. Z-stack images
222 were acquired using 0.5µm (20x objective) or 0.3µm (63x objective) step size. Images were
223 processed using Zen software from Zeiss.
224 G/F-actin in whole-mount confocal images was quantified using FIJI software. Briefly,
225 single optical slice images from the mid-region of full z-stack tendon images were analyzed. A
226 rectangular region of interest (ROI) was selected at the center of the images and channels
227 (red/green/blue) were then separated. The fluorescent intensities within the ROI for each channel
228 were measured. The fluorescent intensity in the green (DNAse-I) channels were divided by the
229 fluorescent intensity in the red (Phalloidin) channels to obtain DNAse-I/Phalloidin (G/F-actin)
230 ratios. Finally, the G/F-actin ratios obtained from each ROI were normalized to the average G/F-
231 actin control values (control averages were set to 1). Of note, tendons from control and stress-

232 deprived groups were stained using identical conditions simultaneously, images were acquired
233 using the same settings on the same day, and ROIs were equivalent in size.
234
235 *Statistical analysis*
236 Each experiment was replicated at least three times on separate occasions. Data from
237 individual experiments were expressed as a percentage of the control average, which was set to
238 100. Graphpad Prism 9 (San Diego, CA, USA) was used for statistical analysis. Outliers in pooled
239 data points were identified using the ROUT method with a maximum desired false discovery rate
240 (Q) set at 1% [52]. Differences between two groups of data were detected using unpaired t-tests.
241 Differences between several experimental groups against a control were detected using analysis of
242 variance followed by Dunnett post hoc tests.
243
244
245

246 **Results**

247 ***Tendon stress deprivation results in tendinosis-like gene changes***

248 Tendinosis progression is characterized by decrease in tenogenic gene expression, an
249 upregulation of degradative genes, and ectopic expression of cartilage genes [27-36, 53-55].
250 Tendon stress deprivation, *in vitro*, has been shown to recapitulate several aspects of tendinosis

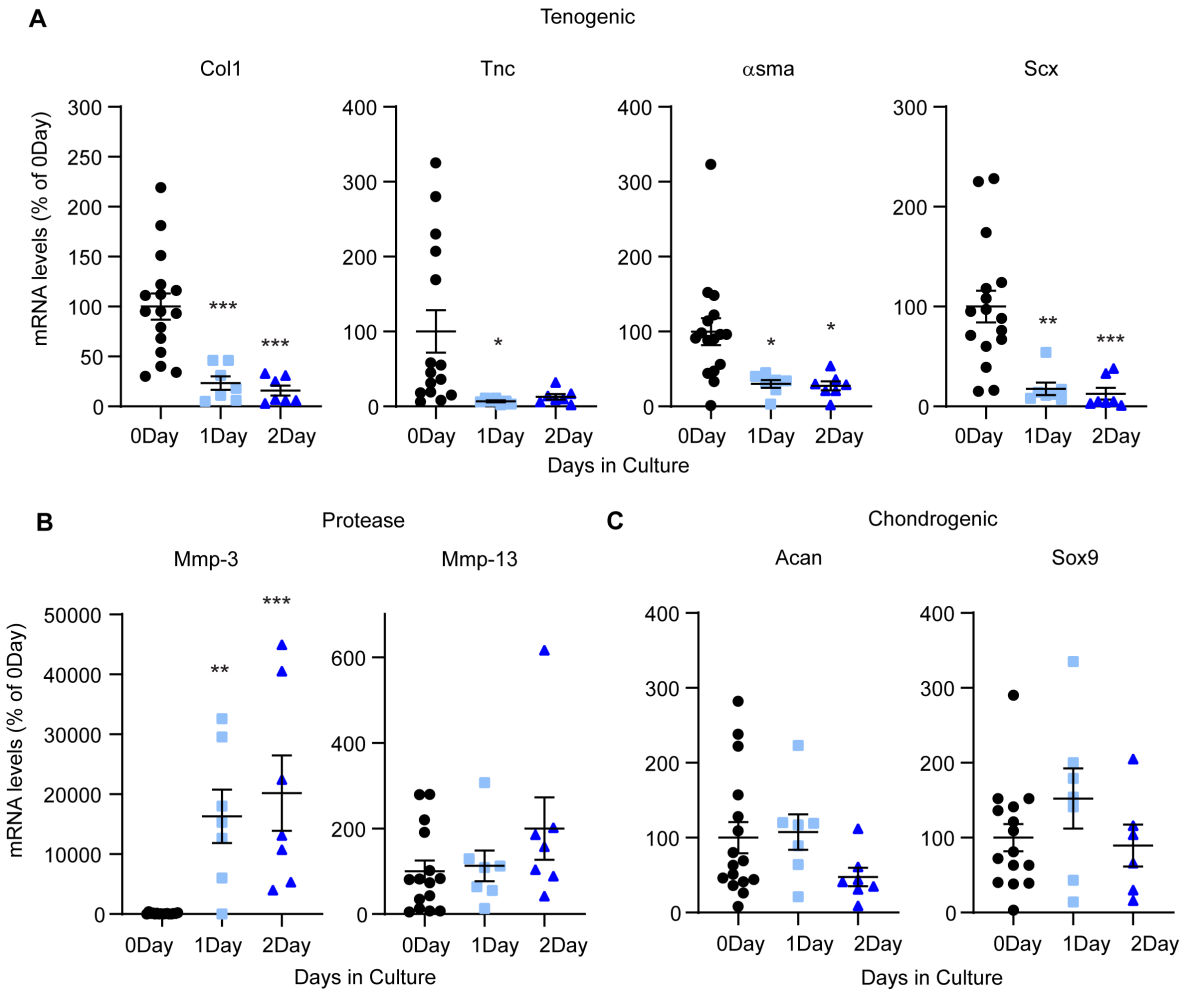

Figure 1. Stress deprivation recapitulates aspects of tendinosis gene expression. Relative real-time PCR of tendons in 1 or 2 day stress deprivation culture as compared to freshly isolated (0 day) tendons demonstrating (A) a reduction in tenogenic marker mRNA levels, (B) an increase in MMP-3 mRNA levels, and (C) no change in chondrogenic mRNA levels. Specific mRNA levels were normalized to Gapdh and normalized values are expressed as a percent of freshly isolated (0 day) controls. *, $p < 0.05$; **, $p < 0.01$; ***, $p < 0.001$

251 gene modulation. We evaluated the effect of stress deprivation on tail tenocyte gene expression by
252 culturing mouse tail tendon fascicles in the absence of stretch for up to 2 days.

253 Stress deprivation decreases tenogenic mRNA levels (Figure 1A). We observe a decrease
254 in Col1, the predominant collagen expressed in tendon [54, 56, 57]; and a decrease in tenascin C
255 (Tnc), a mechanosensitive matricellular glycoprotein present in tendon matrix that assists in the
256 structural arrangement of collagen fibers as well as provides for tissue elasticity [12, 56, 58]. In
257 addition, we observe a reduction in Scleraxis (Scx), a transcription factor that drives the tenogenic
258 expression, such as the expression of collagen-I [59, 60]. Finally, we detect a decrease in alpha-
259 smooth muscle actin (αsma), an actin isoform present in tendon cells, which is thought to be
260 necessary for recovery of tendon cells following stretch [54].

261 Stress deprivation enhances the expression of specific degradative molecules (Figure 1B).
262 Mmp-3 and Mmp-13 have been implicated in tendinosis and are upregulated during stress
263 deprivation [13, 23, 30, 35, 57, 61]. We determine that Mmp-3 is upregulated 163.1-fold by day
264 1 and 201.9-fold by day 2 (Figure 1B). Unlike previous studies [30], we did not observe an increase
265 in Mmp-13 mRNA levels at 1- or 2-days post culture.

266 An increase in chondrogenic expression is a feature of tendinosis [55] but is not
267 recapitulated by tendon stress deprivation. We observed no significant effect on chondrogenic
268 (Acan or Sox9; Figure 1C) mRNA levels up to 2 days of stress deprivation (Figure 1C). Thus, *in*
269 *vitro* stress deprivation of tail tendons recapitulates certain, but not all, aspects of tendinosis.

270

271 ***Stress deprivation promotes cell rounding and destabilizes tenocyte F-actin***

272 We found that tendon stress deprivation alters tenocyte morphology and F-actin
273 depolymerization [6, 11, 13]. To determine if F-actin depolymerization occurs in native tendons,

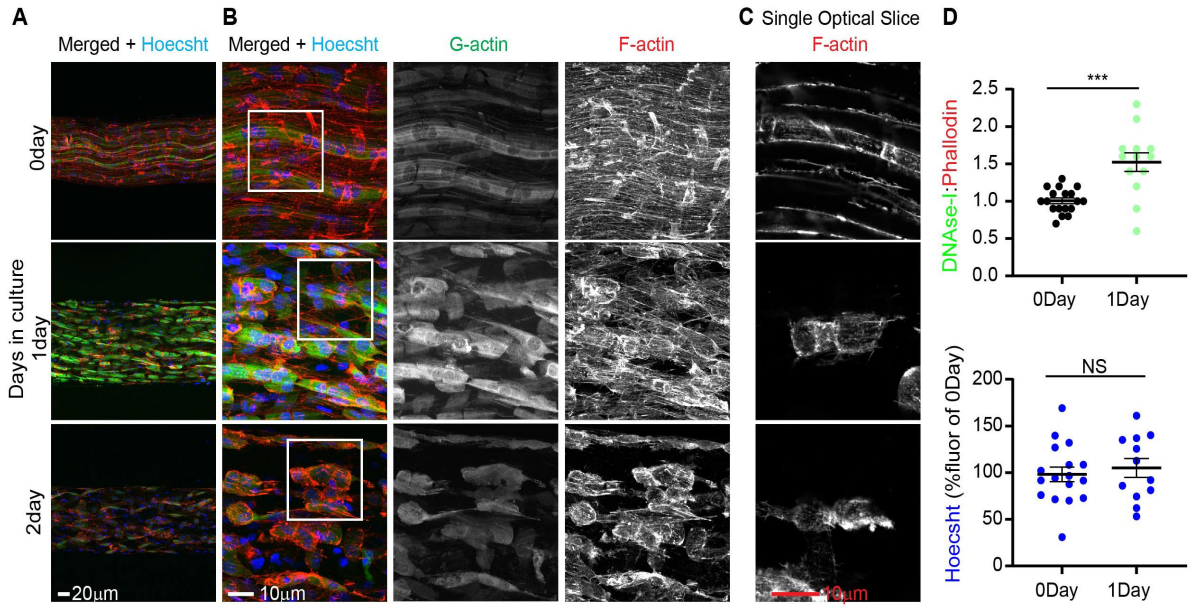

Figure 2. Stress deprivation alters tendon cell morphology and destabilizes F-actin. (A-B) Maximum intensity projections images of tendons demonstrating an increase in G/F-actin staining after 1 day of culture taken with either a 20x (panel A) or 63x (panel B) objective. In panel B, gray scale images represent individual channels for G- and F-actin. (C) Single optical slice of boxed region in panel B, demonstrates that cell morphology and F-actin are altered by stress deprivation. (D) Dot plots of DNAseI:Phalloidin to demonstrate an increase in G/F-actin. Average DNAseI:Phallodin for controls were set to 1.0 and 1 day stress deprived values were scaled accordingly. Nuclei staining intensity using Hoechst was calculated to demonstrate there were no significant differences in staining between control and stress deprived tendons. Average fluorescent intensity for controls were set to 100% and stress deprived tendon intensities were expressed as a relative percentage to controls. ***, $p < 0.001$

274 we performed whole-mount imaging of tendons stained with DNAse-I and Phalloidin to visualize
275 G-and F-actin, respectively. Tendon cells from freshly isolated tendons are elongated and have
276 parallel F-actin networks regarded as stress fibers throughout the tissue [14] (Figure 2A, B). Stress
277 deprivation results in rounded tendon cells. We also observe repression of stress fiber organization.
278 Fluorescent image quantification reveals that stress deprivation elevates G/F-actin staining after
279 one day compared to freshly isolated controls (Figure 2C). By two days of culture, despite

280 differences in F-actin network organization, G/F-actin status is similar to controls (data not
281 shown). Our findings confirm that stress deprivation destabilizes F-actin.

282 These results support the idea that F-actin destabilization regulates tendinosis gene
283 changes. Tpms are known master regulators of F-actin, therefore we next focused on characterizing
284 the role of Tpms in tendon cells.

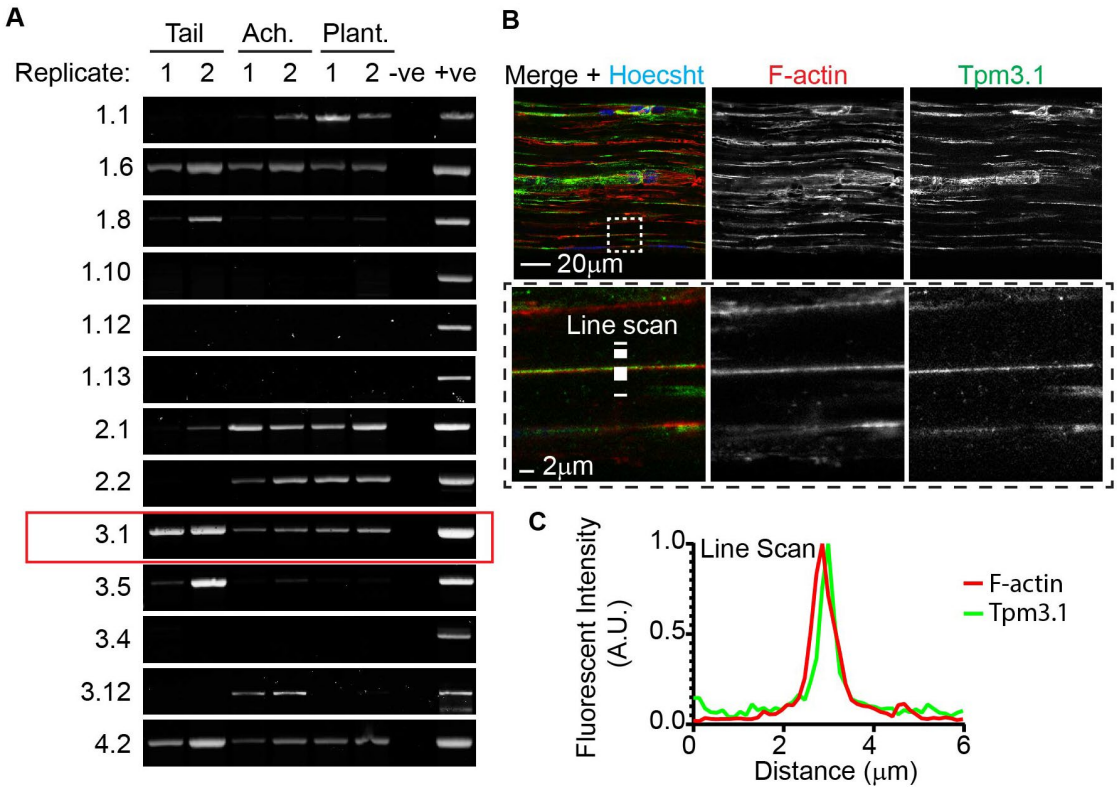

Figure 3. Tpm isoform expression is dependent on tendon type, but all three types examined express Tpm3.1. (A) Semi-quantitative PCR for Tpms in native tail, Achilles (Ach.), and plantaris (Plant.) tendons. (B, top panels) Whole mount immunostaining shows distribution of Tpm3.1 throughout tail tendon. (B, bottom panels) High magnification images of dashed area shows association of Tpm3.1 along F-actin. (C) Line scan analysis showing co-localization of Tpm3.1 with F-actin.

285

286

287

288 ***Tpm Expression in Native Tendon cells***

289 Tpm isoforms have the unique ability to stabilize specific F-actin networks [42, 46, 62,
290 63]. Therefore, we first sought to determine which Tpm isoforms are expressed by tendon cells.
291 Tpm expression is variable and dependent on tendon type. To determine specific Tpm isoform
292 expression within various tendon types (tail, Achilles, and plantaris) tendons, we used semi-
293 quantitative RT-PCR analysis, followed by Sanger Sequencing of cDNA products. Collectively,
294 in total, we found that tendons express 9 Tpm isoforms: Tpm1.1, 1.6, 1.8, 2.1, 2.2, 3.1, 3.5, 3.12,
295 and 4.2. However, the specific Tpms expressed are dependent on tendon type. Only three of the
296 nine Tpm isoforms are consistently expressed in all three tendon types tested: Tpm1.6, 3.1, and
297 4.2.

298 In this study we chose to focus on the regulation of F-actin networks by Tpm3.1, as we
299 previously have shown it to regulate stress fibers in lens epithelial cells [38]. Furthermore, there
300 are established inhibitors toward Tpm3.1, including TR100 [64, 65]. To confirm Tpm 3.1 protein
301 expression and association with F-actin, we performed whole-mount immunostaining of the tail
302 fascicle using antibody 2G10.2 (Table 2) which recognizes the 9D exon of Tpm3.1. Our findings
303 indicate Tpm 3.1 expression within native tail tendon cells. Furthermore, line scan analysis shows
304 overlap in signal between Tpm3.1 and phalloidin staining, suggesting that Tpm3.1 associates with
305 native F-actin stress fibers (Figure 3C).

306

307 ***Inhibition of Tpm3.1 with TR100 alters tenocyte morphology***

308 To determine Tpm3.1 function in tendon cells, we used primary tendon cells isolated from
309 tail tendon fascicles. Primary tendon cells retain stress fiber organization of F-actin [14].

310 Furthermore, cultured cells devoid of matrix are more amenable to biochemical assays (i.e., Triton-
311 based cellular fractionation) than native tissues.

312 We exposed cultured tendon cells to TR100, a small molecule inhibitor that prevents end-
313 to-end assembly of Tpm and reduces Tpm binding along F-actin [64, 66]. Live/dead staining
314 (Figure 4A) and propidium iodide exclusion assay (Figure 4B) demonstrate that treating tendon
315 cells with ≤5uM of TR100 retains cell viability. To determine the effect of Tpm3.1 inhibition on
316 cell morphology, we performed light microscopy followed by image quantification (Figure 4C).
317 Both 2μM and 5μM TR100 decrease overall cell area (Figure 4D). Interestingly, while 2μM
318 TR100 induces tenocyte elongation (decrease in circularity), exposure to 5μM TR100 causes cell
319 rounding (increase in circularity).

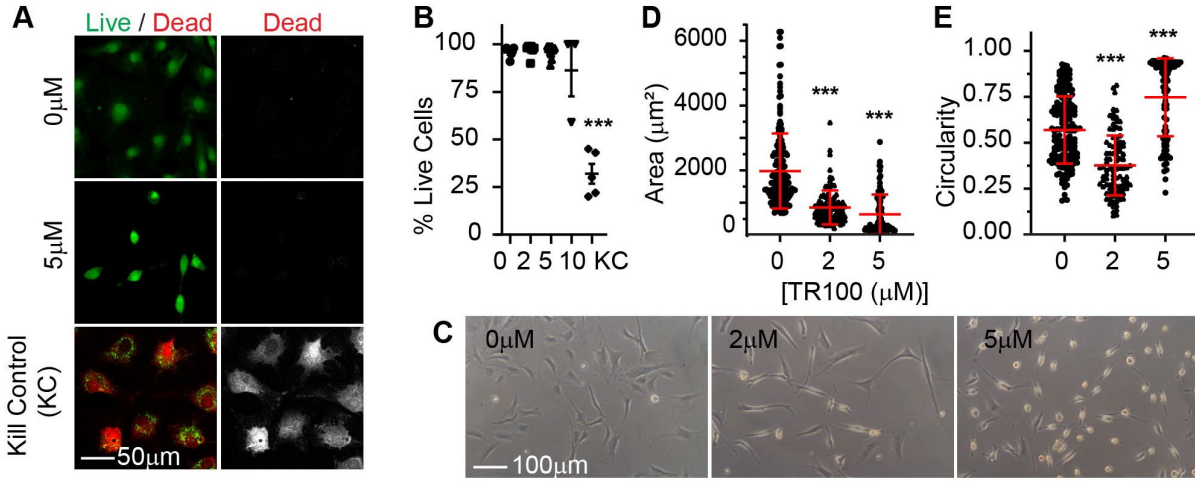

Figure 4. Exposure of cells to TR100 alters tenocyte shape and size. (A) Tendon cells are viable following 1 day treatments of TR100 up to 5mM as seen by positive staining for live cell stain (Calcein AM; green) and negative staining for dead cell stain (Propidium Iodide; red). Cells fixed in 70%EtOH for 15 minutes served as dead controls (Kill control; KC). (B) Dot-plot showing the percentage of cells that are alive following treatments as measured by propidium iodide exclusion counts. (C) Light microscopy images of cells treated with TR100 and corresponding dot-plots demonstrating changes to tenocyte (D) cell area and (E) circularity. ***, $p < 0.001$

320

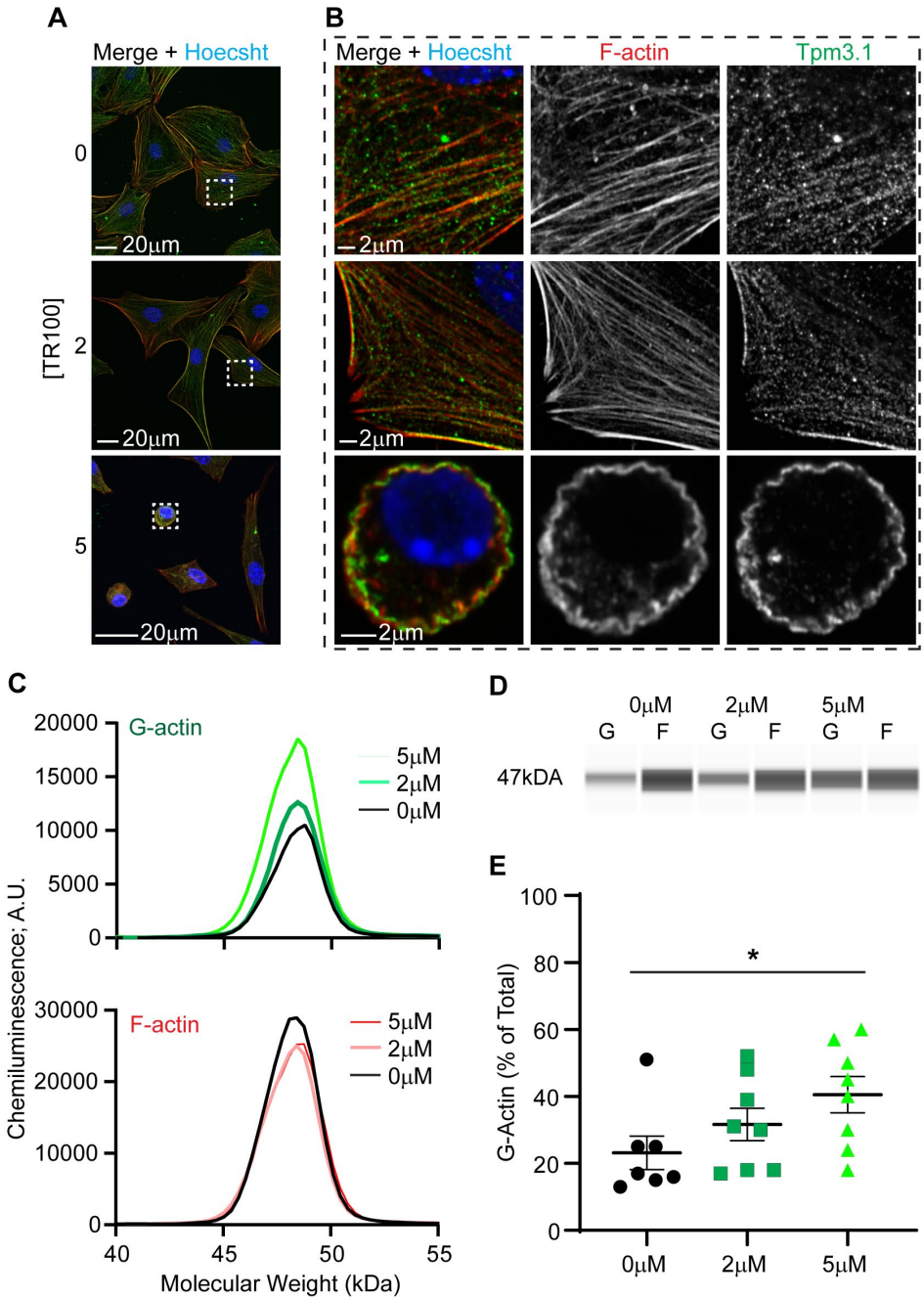

Figure 5. Tpm3.1 inhibition destabilizes F-actin. (A) Maximum intensity projection images of TR100 treated tendon cells, demonstrating that TR100 represses F-actin stress fiber organization. Images taken with a 20x objective. (B) Single optical slice images of boxed regions, demonstrating repression of F-actin stress fibers and acquisition of cortical organization of Tpm3.1 and F-actin (5μM TR100). Images taken with a 63x objective. (C) Capillary western blot (WES) immunoassay electropherogram of Triton-fractionated samples. The triton-soluble fraction is indicative of G-actin (top panel) and the triton-insoluble fraction is indicative of F-actin. (D) Virtual gel showing actin bands at approximately 47kDA. (E) Corresponding dot-plots showing the proportion of G-actin within cells increases by treatment with 5μM TR100. *, $p < 0.05$

322 We sought to determine if Tpm3.1 stabilizes tenocyte F-actin. Confocal microscopy demonstrates
323 that stress fibers are present in cells treated with 2μM TR100 (Figure 5A). However, there appears
324 to be a slight reduction in Tpm3.1 staining along F-actin stress fibers compared to control (Figure
325 5B). Treatment with 5μM TR100 represses F-actin stress fibers and results in cortically arranged
326 Tpm3.1 and F-actin in a subpopulation of cells.

327 Next, we evaluated G/F-actin proportion in TR100 treated cells using Triton-fractionation
328 followed by WES-capillary electrophoresis (Figure 5C-E). Treatment with TR100 increases the
329 amount of actin present in soluble portions indicative of elevated G-actin (Figure 5D, E). On
330 average, there is a significant increase in the proportion of G/F-actin by treatment with 5μM of
331 TR100. While 2μM of TR100 appears to result in a slight increase in the proportion of G/F-actin,
332 this was not statistically significant ($p = 0.42$).

333

334 ***TR100 treatment results in tendinosis-like gene changes***

335 Our findings in Figure 5 reveal that Tpm3.1 regulates F-actin stability in tendon cells. The
336 findings that F-actin destabilization regulates tendinosis-like gene changes, leads to us next testing
337 the hypothesis that Tpm3.1 inhibition will induce downregulation of tenogenic genes and
338 upregulation of chondrogenic and protease expression.

339 We determined that destabilization of F-actin by TR100 treatment decreases tenogenic
340 mRNA levels. This was apparent at both 2μM and 5μM treatments. With 5μM treatment of TR100,
341 there is a 21.2-, 1.4-, 29.2-, 2.5- fold decrease in Col1, Tnc, αsma, and Scx respectively. Treatment
342 with 5μM of TR100 also upregulates chondrogenic mRNA levels resulting in a 3.4- and 9.2-fold
343 increase in Acan and Sox9, respectively. Lastly, exposure of cells to 5μM TR100 upregulates
344 protease expression resulting in an 18.1 and 374.3-fold increase in Mmp-3 and Mmp-13,

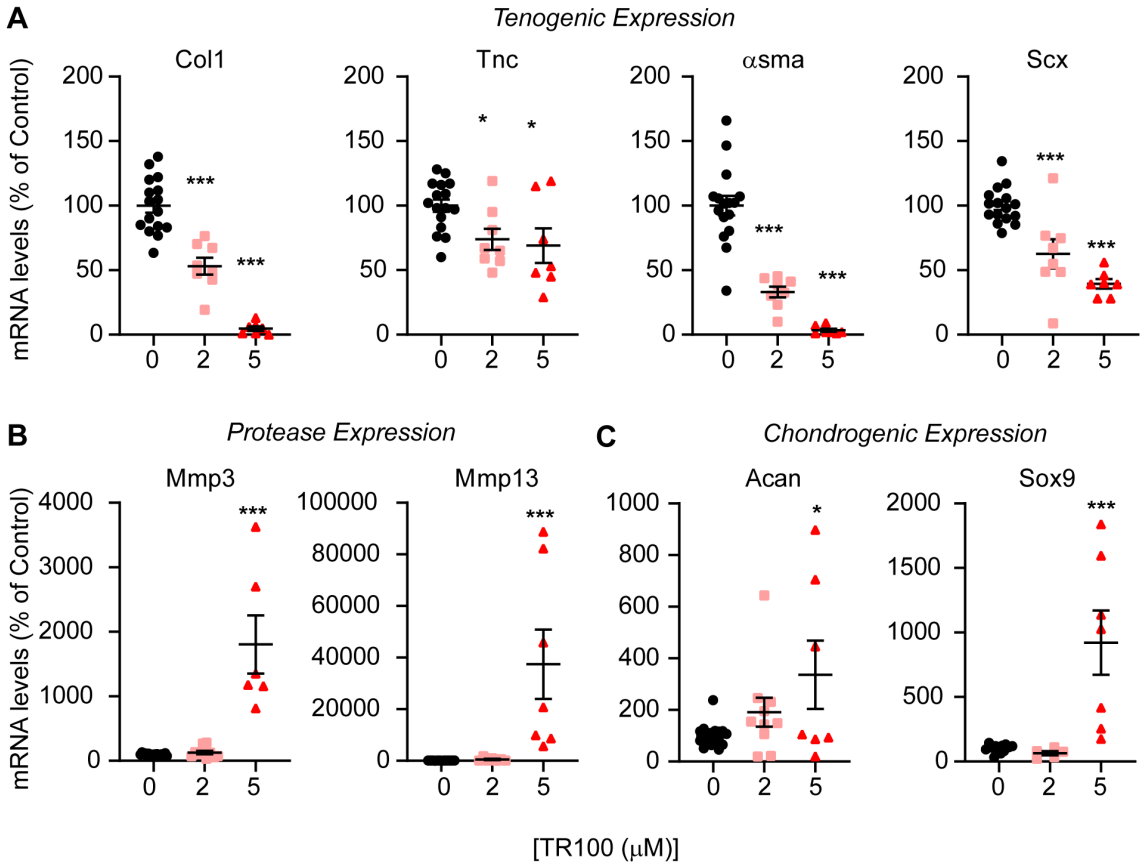

Figure 6. Destabilization of F-actin by inhibition of Tpm3.1 results in tendinosis-like gene modulation. Relative real-time PCR of tendon cells treated with 0, 2, or 5μM TR100 demonstrating (A) a reduction in tenocyte marker mRNA levels, and an (B) increase in protease mRNA levels, and (C) chondrogenic mRNA levels. Specific mRNA levels were normalized to Gapdh and normalized values are expressed as a percent of non-treated (0μM) controls. *, $p < 0.05$; ***, $p < 0.001$

respectively. We found that only the 5μM treatment, but not 2μM treatment, upregulates chondrogenic and protease levels.

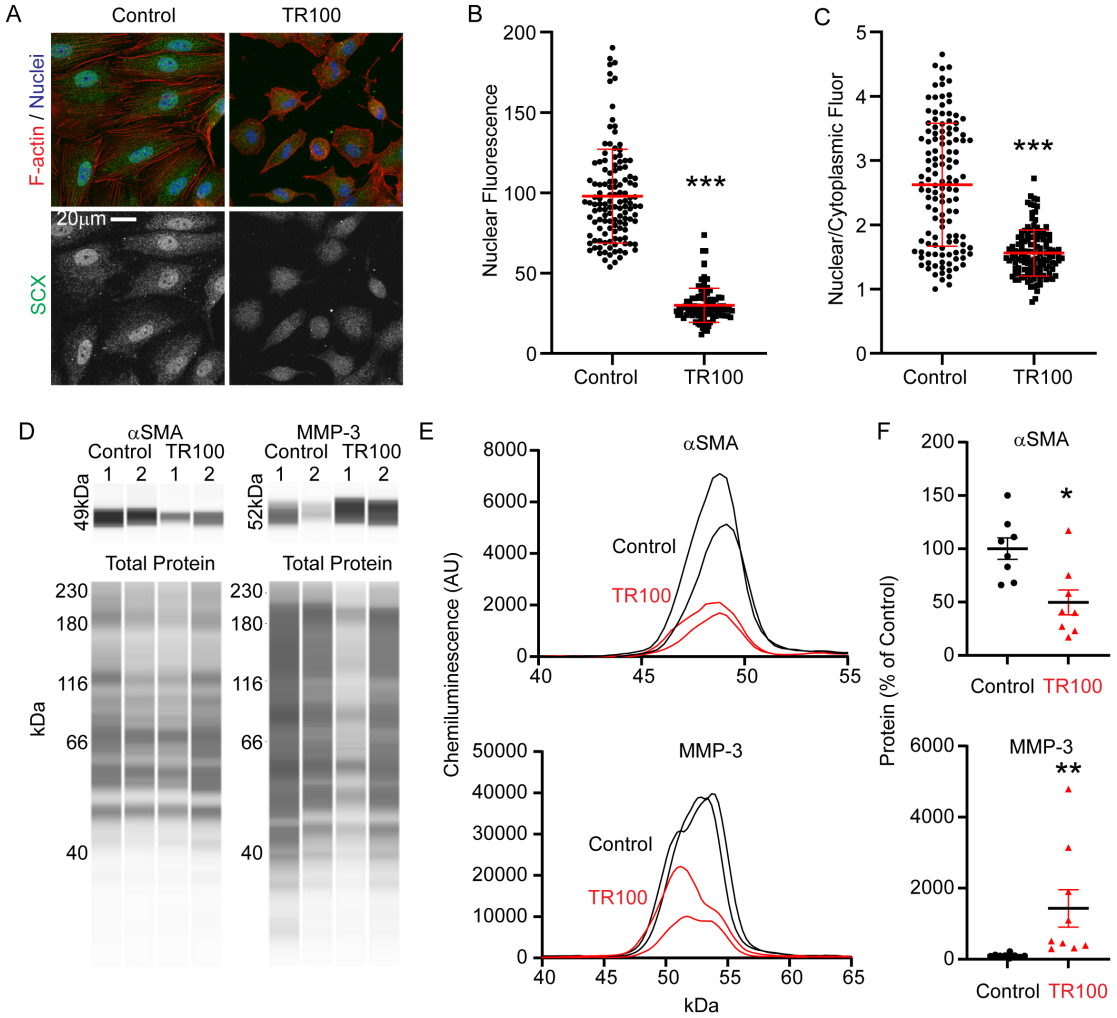

Figure 7. Modulation of select protein levels by TR100 (5μM) treatment. (A) Representative fluorescent confocal microscopy images for SCX. (B) Total nuclear fluorescence for SCX in individual cells, expressed as a percentage of mean nuclear fluorescence of control cells. (C) Calculated nuclear/cytoplasmic ratio of SCX for individual cells. Representative WES electrophoresis data showing (D) pseudo-western blots with corresponding (B) electropherograms for αSMA and MMP-3. (C) αSMA and MMP-3 protein after normalization to total protein. Protein levels were expressed as a percentage of untreated controls. *, $p < 0.05$; **, $p < 0.01$; ***, $p < 0.001$

347 We examined modulation of protein expression by 5μM TR100 treatment on select
348 molecules using immunostaining followed by quantitative image analysis (SCX) or via capillary
349 electrophoresis (αSMA and MMP-3). TR100 decreases the total nuclear fluorescent staining for
350 SCX in tendon cells (Figure 7A, B) as well as the proportion of nuclear/cytosplasmic SCX (Figure
351 7A, C). Additionally, TR100 decreases αSMA protein levels by 2.0-fold (Figures 7D-F). Lastly,
352 TR100 increases MMP-3 protein levels by 14.3-fold (Figure 7D-F). Modulation of SCX, aSMA,
353 and MMP-3 is consistent between mRNA and protein levels.
354

355 **Discussion**

356 This study provides novel insight into the regulation of pathological cellular phenotype by
357 F-actin destabilization. We determined tendinosis-like gene changes caused by stress deprivation
358 coincides with F-actin destabilization. This result led us to investigate the molecular regulation of
359 F-actin stability. We revealed that tendons express several Tpm isoforms, including Tpm3.1, a
360 stress fiber associated Tpm [38, 45, 46]. We found that Tpm3.1 associates with F-actin networks
361 in tendon cells and regulates tenocyte cellular phenotype. Tpm3.1 inhibition destabilizes tenocyte
362 F-actin stress fibers causing a robust tendinosis-like gene response.

363 Our data supports the speculation that stress deprivation regulates cellular phenotype by
364 destabilization of F-actin [37]. Previously it was shown that tendon stress deprivation increases
365 Mmp mRNA levels [28, 37]. It was also demonstrated that stretching *in vitro* cultured tendons can
366 repress Mmp upregulation [28, 37]. Mechanical stretch appears to regulate Mmp expression via
367 actin-based mechanisms as treating stretched tendons with cytochalasin D (an actin
368 depolymerization agent) abrogates the protective effects of stretch [37]. This led to the speculation
369 that stress deprivation regulates Mmp expression via actin depolymerization. However, evidence

370 for F-actin depolymerization in stress deprivation was still required. In the current study, we
371 provide empirical evidence that stress deprivation destabilizes F-actin as demonstrated by an
372 increase in G/F-actin staining (Figure 2). We show this increase in G/F-actin coincides with an
373 increase in protease expression (Mmp-3) (Figure 1). This finding is consistent with our previous
374 findings in bone cells, where stress deprivation of osteoblast-like MG-63 cells in collagen gels
375 enhances Mmp-3 gene expression [61]. Unlike other previous studies, Mmp-13 was not found to
376 be upregulated, although there was a trend toward an increase in Mmp-13 expression by day 2 (p
377 = 0.17). Previous studies examined Mmp expression at later time points (i.e., up to 10 days of
378 stress deprivation) [36] which could explain the discrepancy in Mmp-13 response. Note, we did
379 not examine Mmp-1 expression here, as it is not expressed in mice. Nevertheless, our findings
380 indicate that F-actin destabilization corresponds to an increase in Mmp-3, a protease that plays a
381 role in tendinosis [67]. The destabilization of F-actin is an important regulator of Mmps during
382 disease processes like tendinosis.

383 We determined that tendon cells express several Tpm isoforms, including several known
384 stress fiber-associated Tpms (Figure 3). Previously, Benjamin et al., (2002) indicated the presence
385 of Tpm in tendon cells using Western blotting and immunofluorescence. However, Tpm antibodies
386 are developed using peptides that correspond to specific exons that are highly conserved between
387 various Tpms [63]. Thus, antibodies are specific to exons and not to particular isoforms. The
388 particular (TM311) antibody used by Benjamin et al. recognizes an epitope on exon 1A of Tpm1
389 and 2 [63]. Therefore, it remained unclear which exact Tpm isoform was expressed in tendons. In
390 our present study, we determined that tendon cells can express 9 Tpms: Tpm1.1, 1.6, 1.8, 2.1, 2.2,
391 3.1, 3.5, 3.12, 4.2. Based on our data, Benjamin et al. could have been probing for Tpms 1.1, 1.6,
392 2.1, 2.2. Tpm2.1 has been identified as a stress-fiber associated Tpm [46]. However, it is not

393 present in all tendons, specifically tail tendons. Intriguingly, out of the nine Tpm isoforms
394 expressed by tendon, we found that only three isoforms were consistently expressed in all tendons
395 (tail, Achilles, plantaris) examined Tpm1.6, 3.1, and 4.2. This diversity of Tpm isoform may reflect
396 the formation of specified F-actin networks in different tendon types to meet
397 the unique tendon structures and mechanical functions [47]. Two of these isoforms,
398 Tpm3.1 and 4.2, are known stress-fiber-associated Tpms. We chose to focus on Tpm3.1 as we
399 previously showed it is a crucial regulator of F-actin stress fibers in lens epithelial cells [38]. The
400 present study is the first, to our knowledge, to examine Tpm3.1 in tendon cells.
401 Tpm3.1 associates with F-actin in native tendon cells as well as *in vitro* cultured tendon
402 cells to maintain F-actin stress fibers (Figure 3). The association of Tpm3.1 with stress fibers in
403 tendon cells is in agreement with past studies on lens epithelial cells [38], human osteosarcoma
404 (U2OS) [45, 46, 68, 69], human neuroblastoma (SK-N-BE(2) [70], and neuronal (B35) [62] cells.
405 Tpm3.1 maintains F-actin networks through regulation of other actin associated molecules. It has
406 been shown to promote the activation of non-muscle myosin activity [45, 46, 62, 70] as well as
407 interfere with the association of severing molecules (i.e. cofilin) onto actin [62]. Here, we show
408 that inhibition of Tpm3.1 results in the destabilization of F-actin stress fibers (Figure 5) leading to
409 tendinosis-like molecule modulation (Figure 6 and 7). Surprisingly, as compared to stress
410 deprivation of tendons, Tpm3.1 inhibition by TR100 treatment of cells had a more substantial
411 effect on the genes tested. TR100 treatment not only decreased tenogenic expression but also
412 enhanced chondrogenic genes, consistent with tendinosis [44]. Additionally, while stress
413 deprivation modulated Mmp-3 but not Mmp-13, TR100 increased both Mmp-3 as well as Mmp-
414 13. The greater response by TR100 treatment of cells could indicate the greater level of actin

415 destabilization achieved by directly perturbing actin by TR100 treatment as compared to stress
416 deprivation which may not have as vast an effect on F-actin network organization.

417 It remains unclear how F-actin regulates gene expression in tendon cells. We have shown
418 in chondrocytes and lens cells that F-actin depolymerization can directly regulate gene expression
419 by controlling the cytoplasmic/nuclear shuttling of myocardin related transcription factor (MRTF)
420 [38-40, 71]. The export of MRTF from the nucleus to the cytoplasm, caused by F-actin
421 depolymerization, has been associated with downregulation of Col1, Tnc, and αsma expression as
422 well as upregulation of Sox9 [38-40]. There is limited data that shows the regulation of Scx, Mmp-
423 3, and Mmp-13 by MRTF. However, MRTF has been shown to regulate another Mmp, Mmp-12,
424 in nucleus pulposus cells [72]. Intriguingly, in the present study, we identified a decrease in the
425 nuclear proportion of transcription factor SCX by TR100 treatment. SCX is known to regulate
426 sox9 expression, collagen synthesis, and the myofibroblast phenotype acquisition [60, 73-75].
427 Therefore, the decreased nuclear SCX may explain the upregulation of Sox9 as well as the
428 downregulation of Col1, Tnc, and αsma mRNA levels that we found in the present study. To our
429 knowledge, this is the first study to associate F-actin depolymerization regulation of SCX
430 localization. Future studies are required to determine the mechanisms downstream of F-actin
431 depolymerization that regulate gene expression.

432 Since we demonstrate that F-actin stability is regulated by Tpm3.1, this could lead to the
433 speculation that the Tpm3.1 plays a role in tendinosis. Tendon overuse is often regarded as a cause
434 of tendinosis. It has been suggested that tendon overuse causes a paradoxical stress deprivation of
435 tendon cells [25]. In support of this mechanotransmission paradox, *ex vivo* overloading of rat tail
436 tendon has been shown to result in cellular-matrix disruptions [26]. We speculate cellular-matrix
437 disruption leads to cellular stress deprivation and destabilization of F-actin. We predict Tpm(s) to

438 be involved in F-actin destabilization as Tpms have been shown to be mechanoregulated in tendon
439 cells. Benjamin et al. have shown that *in vitro* mechanical stimulation of tendon cells elevate
440 protein expression of Tpm [14]. Our future studies aim to delineate the role that Tpm3.1 plays in
441 F-actin destabilization by stress deprivation using an *in vivo* model of tendinosis.

442 In conclusion, F-actin is a critical mediator of cellular phenotype and determining the
443 regulation of F-actin networks by Tpms in tissues could lead to new therapeutic interventions that
444 could prevent and/or reverse progression of disease in various tissue types including tendon.

445

446 **Acknowledgements**

447 The authors thank Thomas Manzoni, Grace Emin, and Sofia Gonzalez-Nolde for critical reading
448 of the manuscript. We also thank Sofia Gonzalez-Nolde for technical expertise in designing the
449 real-time RT-PCR primers used in this study. Research reported in this project was supported by
450 University of Delaware Research Fund – Strategic Initiatives (UDRF-SI) grant as well as the
451 Delaware Center for Musculoskeletal Research from the National Institute of Health's National
452 Institute of General Medical Sciences under grant number P20GM139760.

453 **References**

454 [1] J. Hatakeyama, M. Nomura, Y. Wakimoto, S. Inoue, C. Li, D. Takamura, T. Akisue, H. Moriyama, Effects
455 of cyclic tensile strain and microgravity on the distribution of actin fiber and Fat1 cadherin in murine
456 articular chondrocytes, J Biomech 129 (2021) 110774.
457 [2] C. Li, J. Luo, X. Xu, Z. Zhou, S. Ying, X. Liao, K. Wu, Single cell sequencing revealed the underlying
458 pathogenesis of the development of osteoarthritis, Gene 757 (2020) 144939.
459 [3] A. Blangy, G. Bompard, D. Guerit, P. Marie, J. Maurin, A. Morel, V. Vives, The osteoclast cytoskeleton -
460 current understanding and therapeutic perspectives for osteoporosis, J Cell Sci 133(13) (2020).
461 [4] A.I. Garbe, A. Roscher, C. Schuler, A.H. Lutter, M. Glosmann, R. Bernhardt, M. Chopin, U. Hempel, L.C.
462 Hofbauer, S. Rammelt, M. Egerbacher, R.G. Erben, R. Jessberger, Regulation of bone mass and osteoclast
463 function depend on the F-actin modulator SWAP-70, J Bone Miner Res 27(10) (2012) 2085-96.
464 [5] M.D. Gardiner, T.L. Vincent, C. Driscoll, A. Burleigh, G. Bou-Gharios, J. Saklatvala, H. Nagase, A.
465 Chanalaris, Transcriptional analysis of micro-dissected articular cartilage in post-traumatic murine
466 osteoarthritis, Osteoarthritis Cartilage 23(4) (2015) 616-28.
467 [6] M. Lavagnino, K.L. Gardner, S.P. Arnoczky, High magnitude, in vitro, biaxial, cyclic tensile strain induces
468 actin depolymerization in tendon cells, Muscles Ligaments Tendons J 5(2) (2015) 124-8.
469 [7] W. Lee, R.J. Nims, A. Savadipour, Q. Zhang, H.A. Leddy, F. Liu, A.L. McNulty, Y. Chen, F. Guilak, W.B.
470 Liedtke, Inflammatory signaling sensitizes Piezo1 mechanotransduction in articular chondrocytes as a
471 pathogenic feed-forward mechanism in osteoarthritis, Proc Natl Acad Sci U S A 118(13) (2021).
472 [8] X. Li, L. Wang, B. Huang, Y. Gu, Y. Luo, X. Zhi, Y. Hu, H. Zhang, Z. Gu, J. Cui, L. Cao, J. Guo, Y. Wang, Q.
473 Zhou, H. Jiang, C. Fang, W. Weng, X. Chen, X. Chen, J. Su, Targeting actin-bundling protein L-plastin as an
474 anabolic therapy for bone loss, Sci Adv 6(47) (2020).
475 [9] J. Neugebauer, J. Heilig, S. Hosseinibarkooie, B.C. Ross, N. Mendoza-Ferreira, F. Nolte, M. Peters, I.
476 Holker, K. Hupperich, T. Tschanz, V. Grysko, F. Zaucke, A. Niehoff, B. Wirth, Plastin 3 influences bone
477 homeostasis through regulation of osteoclast activity, Hum Mol Genet 27(24) (2018) 4249-4262.
478 [10] K.C. Tsolis, E.S. Bei, I. Papathanasiou, F. Kostopoulou, V. Gkretsi, K. Kalantzaki, K. Malizos, M. Zervakis,
479 A. Tsezou, A. Economou, Comparative proteomic analysis of hypertrophic chondrocytes in osteoarthritis,
480 Clin Proteomics 12(1) (2015) 12.
481 [11] W. Chen, Y. Deng, J. Zhang, K. Tang, Uniaxial repetitive mechanical overloading induces influx of
482 extracellular calcium and cytoskeleton disruption in human tenocytes, Cell Tissue Res 359(2) (2015) 577-
483 587.
484 [12] T.A. Jarvinen, L. Jozsa, P. Kannus, T.L. Jarvinen, T. Hurme, M. Kvist, M. Pelto-Huikko, H. Kalimo, M.
485 Jarvinen, Mechanical loading regulates the expression of tenascin-C in the myotendinous junction and
486 tendon but does not induce de novo synthesis in the skeletal muscle, J Cell Sci 116(Pt 5) (2003) 857-66.
487 [13] M. Lavagnino, S.P. Arnoczky, In vitro alterations in cytoskeletal tensional homeostasis control gene
488 expression in tendon cells, J Orthop Res 23(5) (2005) 1211-8.
489 [14] J.R. Ralphs, A.D. Waggett, M. Benjamin, Actin stress fibres and cell-cell adhesion molecules in
490 tendons: organisation in vivo and response to mechanical loading of tendon cells in vitro, Matrix Biol 21(1)
491 (2002) 67-74.
492 [15] G.M. Thornton, X. Shao, M. Chung, P. Sciore, R.S. Boorman, D.A. Hart, I.K. Lo, Changes in mechanical
493 loading lead to tendonspecific alterations in MMP and TIMP expression: influence of stress deprivation
494 and intermittent cyclic hydrostatic compression on rat supraspinatus and Achilles tendons, Br J Sports
495 Med 44(10) (2010) 698-703.
496 [16] M. Kjaer, H. Langberg, K. Heinemeier, M.L. Bayer, M. Hansen, L. Holm, S. Doessing, M. Kongsgaard,
497 M.R. Krogsgaard, S.P. Magnusson, From mechanical loading to collagen synthesis, structural changes and
498 function in human tendon, Scand J Med Sci Sports 19(4) (2009) 500-10.

[17] K. Mubyana, D.T. Corr, Cyclic Uniaxial Tensile Strain Enhances the Mechanical Properties of Engineered, Scaffold-Free Tendon Fibers, Tissue Eng Part A 24(23-24) (2018) 1808-1817.
[18] V. Fleischhacker, F. Klatte-Schulz, S. Minkwitz, A. Schmock, M. Rummler, A. Seliger, B.M. Willie, B. Wildemann, In Vivo and In Vitro Mechanical Loading of Mouse Achilles Tendons and Tenocytes-A Pilot Study, Int J Mol Sci 21(4) (2020).
[19] P. Sawadkar, D. Player, L. Bozec, V. Mudera, The mechanobiology of tendon fibroblasts under static and uniaxial cyclic load in a 3D tissue engineered model mimicking native extracellular matrix, J Tissue Eng Regen Med 14(1) (2020) 135-146.
[20] T. Wang, Z. Lin, M. Ni, C. Thien, R.E. Day, B. Gardiner, J. Rubenson, T.B. Kirk, D.W. Smith, A. Wang, D.G. Lloyd, Y. Wang, Q. Zheng, M.H. Zheng, Cyclic mechanical stimulation rescues achilles tendon from degeneration in a bioreactor system, J Orthop Res 33(12) (2015) 1888-96.
[21] E. Huisman, A. Lu, R.G. McCormack, A. Scott, Enhanced collagen type I synthesis by human tenocytes subjected to periodic in vitro mechanical stimulation, BMC Musculoskelet Disord 15 (2014) 386.
[22] J. Zhang, J.H. Wang, The effects of mechanical loading on tendons--an in vivo and in vitro model study, PLoS One 8(8) (2013) e71740.
[23] I.K. Lo, L.L. Marchuk, R. Hollinshead, D.A. Hart, C.B. Frank, Matrix metalloproteinase and tissue inhibitor of matrix metalloproteinase mRNA levels are specifically altered in torn rotator cuff tendons, Am J Sports Med 32(5) (2004) 1223-9.
[24] S.P. Arnoczky, M. Lavagnino, M. Egerbacher, The mechanobiological aetiopathogenesis of tendinopathy: is it the over-stimulation or the under-stimulation of tendon cells?, Int J Exp Pathol 88(4) (2007) 217-26.
[25] M. Lavagnino, M.E. Wall, D. Little, A.J. Banes, F. Guilak, S.P. Arnoczky, Tendon mechanobiology: Current knowledge and future research opportunities, J Orthop Res 33(6) (2015) 813-22.
[26] S.J. Ros, P.M. Muljadi, E.L. Flatow, N. Andarawis-Puri, Multiscale mechanisms of tendon fatigue damage progression and severity are strain and cycle dependent, J Biomech 85 (2019) 148-156.
[27] I.K. Lo, L.L. Marchuk, K.E. Leatherbarrow, C.B. Frank, D.A. Hart, Collagen fibrillogenesis and mRNA levels in the maturing rabbit medial collateral ligament and patellar tendon, Connect Tissue Res 45(1) (2004) 11-22.
[28] S.L. Wunderli, J. Widmer, N. Amrein, J. Foolen, U. Silvan, O. Leupin, J.G. Snedeker, Minimal mechanical load and tissue culture conditions preserve native cell phenotype and morphology in tendon-a novel ex vivo mouse explant model, J Orthop Res 36(5) (2018) 1383-1390.
[29] T. Stauber, U. Blache, J.G. Snedeker, Tendon tissue microdamage and the limits of intrinsic repair, Matrix Biol 85-86 (2020) 68-79.
[30] M. Lavagnino, S.P. Arnoczky, M. Egerbacher, K.L. Gardner, M.E. Burns, Isolated fibrillar damage in tendons stimulates local collagenase mRNA expression and protein synthesis, J Biomech 39(13) (2006) 2355-62.
[31] M. Lavagnino, S.P. Arnoczky, E. Kepich, O. Caballero, R.C. Haut, A finite element model predicts the mechanotransduction response of tendon cells to cyclic tensile loading, Biomech Model Mechanobiol 7(5) (2008) 405-16.
[32] S.P. Arnoczky, M. Lavagnino, M. Egerbacher, O. Caballero, K. Gardner, Matrix metalloproteinase inhibitors prevent a decrease in the mechanical properties of stress-deprived tendons: an in vitro experimental study, Am J Sports Med 35(5) (2007) 763-9.
[33] K. Gardner, S.P. Arnoczky, O. Caballero, M. Lavagnino, The effect of stress-deprivation and cyclic loading on the TIMP/MMP ratio in tendon cells: an in vitro experimental study, Disabil Rehabil 30(20-22) (2008) 1523-9.
[34] M. Egerbacher, K. Gardner, O. Caballero, J. Hlavaty, S. Schlosser, S.P. Arnoczky, M. Lavagnino, Stress-deprivation induces an up-regulation of versican and connexin-43 mRNA and protein synthesis and increased ADAMTS-1 production in tendon cells in situ, Connect Tissue Res (2021) 1-10.

547 [35] S.P. Arnoczky, M. Lavagnino, M. Egerbacher, O. Caballero, K. Gardner, M.A. Shender, Loss of
548 homeostatic strain alters mechanostat "set point" of tendon cells in vitro, Clin Orthop Relat Res 466(7)
549 (2008) 1583-91.
550 [36] L. Jafari, M. Savard, F. Gobeil, E. Langelier, Characterization of moderate tendinopathy in ex vivo
551 stress-deprived rat tail tendons, Biomed Eng Online 18(1) (2019) 54.
552 [37] S.P. Arnoczky, T. Tian, M. Lavagnino, K. Gardner, Ex vivo static tensile loading inhibits MMP-1
553 expression in rat tail tendon cells through a cytoskeletally based mechanotransduction mechanism, J
554 Orthop Res 22(2) (2004) 328-33.
555 [38] J. Parreno, M.B. Amadeo, E.H. Kwon, V.M. Fowler, Tropomyosin 3.1 Association With Actin Stress
556 Fibers is Required for Lens Epithelial to Mesenchymal Transition, Invest Ophthalmol Vis Sci 61(6) (2020)
557 2.
558 [39] J. Parreno, S. Raju, M.N. Niaki, K. Andrejevic, A. Jiang, E. Delve, R. Kandel, Expression of type I collagen
559 and tenascin C is regulated by actin polymerization through MRTF in dedifferentiated chondrocytes, FEBS
560 Lett 588(20) (2014) 3677-84.
561 [40] J. Parreno, S. Raju, P.H. Wu, R.A. Kandel, MRTF-A signaling regulates the acquisition of the contractile
562 phenotype in dedifferentiated chondrocytes, Matrix Biol 62 (2017) 3-14.
563 [41] E. Delve, V. Co, S.C. Regmi, J. Parreno, T.A. Schmidt, R.A. Kandel, YAP/TAZ regulates the expression of
564 proteoglycan 4 and tenascin C in superficial-zone chondrocytes, Eur Cell Mater 39 (2020) 48-64.
565 [42] P.W. Gunning, E.C. Hardeman, P. Lappalainen, D.P. Mulvihill, Tropomyosin - master regulator of actin
566 filament function in the cytoskeleton, J Cell Sci 128(16) (2015) 2965-74.
567 [43] J. Premdas, J.B. Tang, J.P. Warner, M.M. Murray, M. Spector, The presence of smooth muscle actin in
568 fibroblasts in the torn human rotator cuff, J Orthop Res 19(2) (2001) 221-8.
569 [44] K.M. Khan, J.L. Cook, F. Bonar, P. Harcourt, M. Astrom, Histopathology of common tendinopathies.
570 Update and implications for clinical management, Sports Med 27(6) (1999) 393-408.
571 [45] S. Tojkander, G. Gateva, G. Schevzov, P. Hotulainen, P. Naumanen, C. Martin, P.W. Gunning, P.
572 Lappalainen, A molecular pathway for myosin II recruitment to stress fibers, Curr Biol 21(7) (2011) 539-
573 50.
574 [46] G. Gateva, E. Kremneva, T. Reindl, T. Kotila, K. Kogan, L. Gressin, P.W. Gunning, D.J. Manstein, A.
575 Michelot, P. Lappalainen, Tropomyosin Isoforms Specify Functionally Distinct Actin Filament Populations
576 In Vitro, Curr Biol 27(5) (2017) 705-713.
577 [47] A.H. Lee, D.M. Elliott, Comparative multi-scale hierarchical structure of the tail, plantaris, and Achilles
578 tendons in the rat, J Anat 234(2) (2019) 252-262.
579 [48] A.H. Lee, S.E. Szczesny, M.H. Santare, D.M. Elliott, Investigating mechanisms of tendon damage by
580 measuring multi-scale recovery following tensile loading, Acta Biomater 57 (2017) 363-372.
581 [49] A.H. Lee, D.M. Elliott, Freezing does not alter multiscale tendon mechanics and damage mechanisms
582 in tension, Ann N Y Acad Sci 1409(1) (2017) 85-94.
583 [50] S.L. Wunderli, U. Blache, A. Beretta Piccoli, B. Niederost, C.N. Holenstein, F.S. Passini, U. Silvan, L.
584 Bundgaard, U. Auf dem Keller, J.G. Snedeker, Tendon response to matrix unloading is determined by the
585 patho-physiological niche, Matrix Biol 89 (2020) 11-26.
586 [51] C. Cheng, R.B. Nowak, M.B. Amadeo, S.K. Biswas, W.K. Lo, V.M. Fowler, Tropomyosin 3.5 protects the
587 F-actin networks required for tissue biomechanical properties, J Cell Sci 131(23) (2018).
588 [52] H.J. Motulsky, R.E. Brown, Detecting outliers when fitting data with nonlinear regression - a new
589 method based on robust nonlinear regression and the false discovery rate, BMC Bioinformatics 7 (2006)
590 123.
591 [53] R. Bell, N.R. Gendron, M. Anderson, E.L. Flatow, N. Andarawis-Puri, A potential new role for
592 myofibroblasts in remodeling of sub-rupture fatigue tendon injuries by exercise, Sci Rep 8(1) (2018) 8933.
593 [54] M. Chatterjee, P.M. Muljadi, N. Andarawis-Puri, The role of the tendon ECM in mechanotransduction:
594 disruption and repair following overuse, Connect Tissue Res (2021) 1-15.

595 [55] T. Yuan, J. Zhang, G. Zhao, Y. Zhou, C.Q. Zhang, J.H. Wang, Creating an Animal Model of Tendinopathy
596 by Inducing Chondrogenic Differentiation with Kartogenin, PLoS One 11(2) (2016) e0148557.
597 [56] D. Sbardella, G.R. Tundo, G.F. Fasciglione, M. Gioia, S. Bisicchia, E. Gasbarra, E. Ippolito, U. Tarantino,
598 M. Coletta, S. Marini, Role of metalloproteinases in tendon pathophysiology, Mini Rev Med Chem 14(12)
599 (2014) 978-87.
600 [57] P. Sharma, N. Maffulli, Biology of tendon injury: healing, modeling and remodeling, J Musculoskelet
601 Neuronal Interact 6(2) (2006) 181-90.
602 [58] M. Nemoto, K. Kizaki, Y. Yamamoto, T. Oonuma, K. Hashizume, Tenascin-C Expression in Equine
603 Tendon-derived Cells During Proliferation and Migration, J Equine Sci 24(2) (2013) 17-24.
604 [59] R.A. Bagchi, M.P. Czubryt, Synergistic roles of scleraxis and Smads in the regulation of collagen
605 1alpha2 gene expression, Biochim Biophys Acta 1823(10) (2012) 1936-44.
606 [60] V. Lejard, G. Brideau, F. Blais, R. Salingcarnboriboon, G. Wagner, M.H. Roehrl, M. Noda, D. Duprez, P.
607 Houillier, J. Rossert, Scleraxis and NFATc regulate the expression of the pro-alpha1(I) collagen gene in
608 tendon fibroblasts, J Biol Chem 282(24) (2007) 17665-75.
609 [61] J. Parreno, G. Buckley-Herd, I. de-Hemptinne, D.A. Hart, Osteoblastic MG-63 cell differentiation,
610 contraction, and mRNA expression in stress-relaxed 3D collagen I gels, Mol Cell Biochem 317(1-2) (2008)
611 21-32.
612 [62] N.S. Bryce, G. Schevzov, V. Ferguson, J.M. Percival, J.J. Lin, F. Matsumura, J.R. Bamburg, P.L. Jeffrey,
613 E.C. Hardeman, P. Gunning, R.P. Weinberger, Specification of actin filament function and molecular
614 composition by tropomyosin isoforms, Mol Biol Cell 14(3) (2003) 1002-16.
615 [63] G. Schevzov, S.P. Whittaker, T. Fath, J.J. Lin, P.W. Gunning, Tropomyosin isoforms and reagents,
616 Bioarchitecture 1(4) (2011) 135-164.
617 [64] T.T. Bonello, M. Janco, J. Hook, A. Byun, M. Appaduray, I. Dedova, S. Hitchcock-DeGregori, E.C.
618 Hardeman, J.R. Stehn, T. Bocking, P.W. Gunning, A small molecule inhibitor of tropomyosin dissociates
619 actin binding from tropomyosin-directed regulation of actin dynamics, Sci Rep 6 (2016) 19816.
620 [65] A.J. Kee, J. Chagan, J.Y. Chan, N.S. Bryce, C.A. Lucas, J. Zeng, J. Hook, H. Treutlein, D.R. Laybutt, J.R.
621 Stehn, P.W. Gunning, E.C. Hardeman, On-target action of anti-tropomyosin drugs regulates glucose
622 metabolism, Sci Rep 8(1) (2018) 4604.
623 [66] J.R. Stehn, N.K. Haass, T. Bonello, M. Desouza, G. Kottyan, H. Treutlein, J. Zeng, P.R. Nascimento, V.B.
624 Sequeira, T.L. Butler, M. Allanson, T. Fath, T.A. Hill, A. McCluskey, G. Schevzov, S.J. Palmer, E.C. Hardeman,
625 D. Winlaw, V.E. Reeve, I. Dixon, W. Weninger, T.P. Cripe, P.W. Gunning, A novel class of anticancer
626 compounds targets the actin cytoskeleton in tumor cells, Cancer Res 73(16) (2013) 5169-82.
627 [67] S.M. Raleigh, L. van der Merwe, W.J. Ribbans, R.K. Smith, M.P. Schwellnus, M. Collins, Variants within
628 the MMP3 gene are associated with Achilles tendinopathy: possible interaction with the COL5A1 gene, Br
629 J Sports Med 43(7) (2009) 514-20.
630 [68] S. Zhao, J. Cai, X. Zhang, J. Cui, Y. Jiu, Different formins restrict localization of distinct tropomyosins
631 on dorsal stress fibers in osteosarcoma cells, Cytoskeleton (Hoboken) 77(1-2) (2020) 16-24.
632 [69] J.C.M. Meiring, N.S. Bryce, M. Lastra Cagigas, A. Benda, R.M. Whan, N. Ariotti, R.G. Parton, J.H. Stear,
633 E.C. Hardeman, P.W. Gunning, Colocation of Tpm3.1 and myosin IIa heads defines a discrete subdomain
634 in stress fibres, J Cell Sci 132(15) (2019).
635 [70] S. Pathan-Chhatbar, M.H. Taft, T. Reindl, N. Hundt, S.L. Latham, D.J. Manstein, Three mammalian
636 tropomyosin isoforms have different regulatory effects on nonmuscle myosin-2B and filamentous beta-
637 actin in vitro, J Biol Chem 293(3) (2018) 863-875.
638 [71] J. Parreno, V.J. Bianchi, C. Sermer, S.C. Regmi, D. Backstein, T.A. Schmidt, R.A. Kandel, Adherent
639 agarose mold cultures: An in vitro platform for multi-factorial assessment of passaged chondrocyte
640 redifferentiation, J Orthop Res 36(9) (2018) 2392-2405.

641 [72] M. Song, Y. Zhang, Y. Sun, M. Kong, S. Han, C. Wang, Y. Wang, D. Xu, Q. Tu, K. Zhu, C. Sun, G. Li, H.
642 Zhao, X. Ma, Inhibition of RhoA/MRTF-A signaling alleviates nucleus pulposus fibrosis induced by
643 mechanical stress overload, Connect Tissue Res (2021) 1-16.
644 [73] L. Espira, L. Lamoureux, S.C. Jones, R.D. Gerard, I.M. Dixon, M.P. Czubryt, The basic helix-loop-helix
645 transcription factor scleraxis regulates fibroblast collagen synthesis, J Mol Cell Cardiol 47(2) (2009) 188-
646 95.
647 [74] P.L. Roche, R.S. Nagalingam, R.A. Bagchi, N. Aroutiounova, B.M. Belisle, J.T. Wigle, M.P. Czubryt, Role
648 of scleraxis in mechanical stretch-mediated regulation of cardiac myofibroblast phenotype, Am J Physiol
649 Cell Physiol 311(2) (2016) C297-307.
650 [75] T. Furumatsu, C. Shukunami, M. Amemiya-Kudo, H. Shimano, T. Ozaki, Scleraxis and E47 cooperatively
651 regulate the Sox9-dependent transcription, Int J Biochem Cell Biol 42(1) (2010) 148-56.

652